AD-A053 086 NATIONAL BUREAU OF STANDARDS WASHINGTON DC SURFACE S--ETC F/G 7/4
THE ADSORPTION OF CYCLOPARAFFINS ON RU(001) AS STUDIED BY TEMPE--ETC(U)
APR 78 T E MADEY, J T YATES N00014-78-F-0008

UNCLASSIFIED TR-6 NL

1 OF 1
ADA
053086

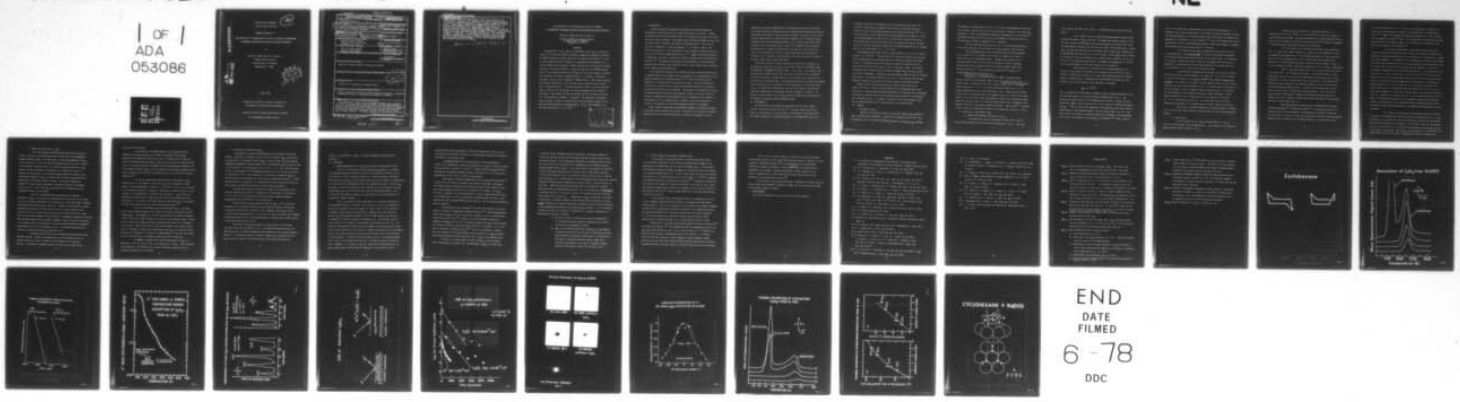

END
DATE
FILMED
6-78
DDC

OFFICE OF NAVAL RESEARCH

Contract N00014-78-F-0008

TECHNICAL REPORT NO. 6

THE ADSORPTION OF CYCLOPARAFFINS ON Ru(001) AS STUDIED BY TEMPERATURE PROGRAMMED DESORPTION AND ELECTRON STIMULATED DESORPTION

by

Theodore E. Madey and John T. Yates, Jr.

Surface Science Division

National Bureau of Standards

Washington, DC 20234

7 April 1978

To be published in Surface Science

UNCLASSIFIED

SECURITY CLASSIFICATION OF THIS PAGE (When Data Entered)

(14) TR-6

REPORT DOCUMENTATION PAGE

READ INSTRUCTIONS BEFORE COMPLETING FORM

1. REPORT NUMBER: Technical Report No. 6
2. GOVT ACCESSION NO.
3. RECIPIENT'S CATALOG NUMBER

4. TITLE (and Subtitle): (6) The Adsorption of Cycloparaffins on Ru(001) as Studied by Temperature Programmed Desorption and Electron Stimulated Desorption.
5. TYPE OF REPORT & PERIOD COVERED: (9) Interim rept.;
6. PERFORMING ORG. REPORT NUMBER

7. AUTHOR(s): (10) Theodore E. Madey, John T. Yates, Jr.
8. CONTRACT OR GRANT NUMBER(s): (15) NØØ014-78-F-ØØØ8 / NØØ014-78-0008 new

9. PERFORMING ORGANIZATION NAME AND ADDRESS
Surface Science Division
National Bureau of Standards
Washington, DC 20234
10. PROGRAM ELEMENT, PROJECT, TASK AREA & WORK UNIT NUMBERS

11. CONTROLLING OFFICE NAME AND ADDRESS
Office of Naval Research
Physical Program Office
Arlington, VA 22217
(11) 7 Apr 78
12. REPORT DATE: April 7, 1978
13. NUMBER OF PAGES: (12) 36p.

14. MONITORING AGENCY NAME & ADDRESS (if different from Controlling Office)
15. SECURITY CLASS. (of this report): Unclassified
15a. DECLASSIFICATION/DOWNGRADING SCHEDULE

16. DISTRIBUTION STATEMENT (of this Report)

Approved for Public Release; Distribution Unlimited.

17. DISTRIBUTION STATEMENT (of the abstract entered in Block 20, if different from Report)

18. SUPPLEMENTARY NOTES

Preprint; to be published in Surface Science.

19. KEY WORDS (Continue on reverse side if necessary and identify by block number)

Surface, adsorption, desorption, electron stimulated desorption, temperature programmed desorption, cycloparaffins, ruthenium, cyclohexane.

20. ABSTRACT (Continue on reverse side if necessary and identify by block number)

The adsorption of C_2H_6, and the cycloparaffins C_3H_6, C_6H_{12}, and C_8H_{16} on Ru(001) at 80 K has been studied using LEED, temperature programmed desorption, and ESDIAD (Electron Stimulated Desorption Ion Angular Distributions). An aim of these studies has been to examine the relationship between ESDIAD ion desorption angles and bond angles in weakly adsorbed species having known internal structure. Fractional monolayers of C_2H_6 and C_3H_6 both yield

(Continued on reverse side)

DD FORM 1 JAN 73 1473 EDITION OF 1 NOV 65 IS OBSOLETE S/N 0102-014-6601

Unclassified
SECURITY CLASSIFICATION OF THIS PAGE (When Data Entered)

410 655

Block 20 (Continued)

ESDIAD patterns due to H^+ ions desorbed in wide cones centered on the surface normal, consistent with adsorption into mobile, disordered layers. In contrast, a fractional monolayer of C_6H_{12} yields a hexagonal H^+ ESDIAD pattern. These results indicate the azimuthal orientation of the C-H bonds and are consistent with a simple model of C_6H_{12} adsorption. In thermal desorption studies, the weakly adsorbed layer in contact with the substrate is easily distinguished from condensed multilayers. Mass analysis of ESD ions reveals that the only ESD ion product is H^+ for hydrocarbon coverages < 1 monolayer. For multilayers of adsorbed C_6H_{12} and C_8H_{16}, the ESD ion products have a mass distribution similar to the gas phase mass spectrometer cracking pattern. For all these fragments, the ESD cross sections are ~~$\sim 2 \times 10^{-17}$ cm^2~~.

approx. = $\sigma > 2 \times 10$ to the -17th power sq cm

THE ADSORPTION OF CYCLOPARAFFINS ON Ru(001) AS STUDIED BY TEMPERATURE PROGRAMMED DESORPTION AND ELECTRON STIMULATED DESORPTION

Theodore E. Madey and John T. Yates, Jr.

Surface Processes and Catalysis Section
National Bureau of Standards
Washington, DC 20234

ABSTRACT

The adsorption of C_2H_6, and the cycloparaffins C_3H_6, C_6H_{12}, and C_8H_{16} on Ru(001) at 80 K has been studied using LEED, temperature programmed desorption, and ESDIAD (Electron Stimulated Desorption Ion Angular Distributions). An aim of these studies has been to examine the relationship between ESDIAD ion desorption angles and bond angles in weakly adsorbed species having known internal structure. Fractional monolayers of C_2H_6 and C_3H_6 both yield ESDIAD patterns due to H^+ ions desorbed in wide cones centered on the surface normal, consistent with adsorption into mobile, disordered layers. In contrast, a fractional monolayer of C_6H_{12} yields a hexagonal H^+ ESDIAD pattern. These results indicate the azimuthal orientation of the C-H bonds and are consistent with a simple model of C_6H_{12} adsorption. In thermal desorption studies, the weakly adsorbed layer in contact with the substrate is easily distinguished from condensed multilayers. Mass analysis of ESD ions reveals that the only ESD ion product is H^+ for hydrocarbon coverages < 1 monolayer. For multilayers of adsorbed C_6H_{12} and C_8H_{16}, the ESD ion products have a mass distribution similar to the gas phase mass spectrometer cracking pattern. For all these fragments, the ESD cross sections are $\gtrsim 2 \times 10^{-17} cm^2$.

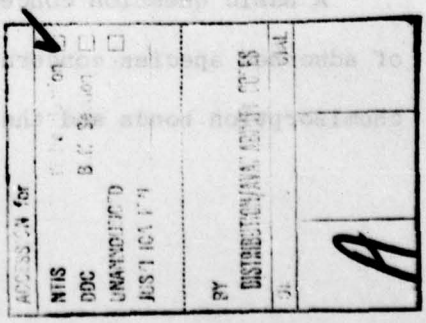

I. INTRODUCTION

A central problem in the physics and chemistry of surfaces concerns the determination of adsorption sites for atoms and molecules on surfaces. Whether an adsorbed atom sits atop a surface atom or in a multiply coordinated site cannot usually be easily determined. Low energy electron diffraction (LEED) has been used in several cases to determine the location of binding sites,[1] but the interpretation of LEED data is sometimes ambiguous.[2] In addition, LEED is frequently not sensitive to the configuration of low Z ligands in adsorbed molecules, such as the H atoms in chemisorbed HC≡CH on Pt.[3] Angular resolved photoemission is beginning to be applied to studies of molecular orientation and conformation at surfaces.[4,5] This method offers promise for determination of local molecular geometry under conditions when diffraction effects from a single crystal substrate do not confound the interpretations.

It has been shown recently that the method of Electron Stimulated Desorption Ion Angular Distributions (ESDIAD) also has potential for the determination of the bonding conformations of adsorbed species.[6,7,8] When an adsorbed layer is bombarded by a focussed beam of low energy electrons ($\sim$ 100 eV) the desorption of positive ions, ground state neutrals, and metastable species can be induced by electronic excitation of the adsorbate. The positive ions liberated by electron stimulated desorption (ESD) have been observed to desorb in discrete "cones" of emission, in symmetric patterns generally having the symmetry of the substrate. The desorption of ions in narrow cones of emission in specific directions is related to the formation of localized chemisorption bonds at the surface.

A basic question concerning the usefulness of ESDIAD for studying structures of adsorbed species concerns the relation between the actual direction of surface chemisorption bonds and the observed angle of positive ion emission. We are

examining this question experimentally by studying the adsorption of molecules (physisorbed and weakly chemisorbed species) having adsorption geometries which are predictable on the basis of their molecular structure. The idea is to see if the resultant ESDIAD pattern is characterized by symmetry and ion desorption angles consistent with the known adsorbate geometry. In a recent study of H_2O and NH_3 adsorbed on the close packed Ru(001) surface,[8] the ESDIAD results indicated that adsorption is largely non-dissociative, and that the O and N atoms are in contact with the substrate with the H atoms pointed away from the substrate. The angle of H^+ ion emission from adsorbed H_2O correlates well with the expected desorption angle based on known bond angles.

In the present work, we report studies of the adsorption of C_2H_6 and the cycloparaffins C_3H_6, C_6H_{12} and C_8H_{16} on the Ru(001) surface using ESDIAD, LEED, and Temperature Programmed Desorption (TPD). In all cases, it was expected that the adsorption energies would be low, and that the molecules would be adsorbed with the carbon skeleton roughly parallel to the surface so as to maximize the interaction with substrate atoms. The experimental TPD results confirm that bonding is non-dissociative and the species are either physisorbed or very weakly chemisorbed. The LEED results demonstrated that none of the species form adsorbed structures characterized by long range order at coverages $\lesssim$ 1 monolayer. For reasons to be discussed, only the C_6H_{12} revealed an ESDIAD pattern indicative of the presence of azimuthly ordered adsorbate species.

II. EXPERIMENTAL

The experimental uhv apparatus and procedures used for these studies have been described in detail previously.[7] The basal plane of hcp Ru was chosen for study because of its high degree of smoothness at the atomic level. The crystal, mounted on a rotatable manipulator, was cryogenically cooled and

resistively heated and its temperature was continuously variable from ∿ 80 K to 1550 K. The crystal was cleaned by heating in O_2 followed by heating in vacuum to 1550 K; the cleaning procedure has been described previously.[9] All of the adsorption studies reported here were performed with the sample at ∿ 80 K; the hydrocarbon gases were dosed onto the surface from a molecular beam doser which insured that the gas flux directed onto the surface was uniform, and that the direct flux was considerably higher than the random background flux of residual gases in the vacuum chamber ($p \sim 1 \times 10^{-10}$ Torr).

The maximum electron beam current in these studies was 1.5×10^{-7} A (current density $\sim 2 \times 10^{-5}$ A/cm^2). The weak positive ion desorption signals were detected using a hemispherical grid assembly backed by a double microchannel plate (MCP) detector. The ESDIAD patterns were displayed visually by acceleration of the output electrons from the MCP detector onto a fluorescent screen. By reversing potentials, the low energy electron diffraction (LEED) pattern from the surface could also be displayed. A quadrupole mass spectrometer (QMS) was used for residual gas analysis. By turning the QMS ion source off, it could also be used for mass analysis of positive ions produced by electron impact on the adsorbed layer.

Typical electron excitation energies for the ESD studies were in the range 100 to 200 eV: typical electron energies for the LEED measurements were 90 to 200 eV. For most LEED and ESDIAD measurements, the patterns were "compressed" by biasing the sample positively by a potential V_B with respect to the (grounded) first hemispherical grid. The angle of incidence of the electron beam for most ESD and LEED measurements was 52° with respect to the crystal normal.

III. RESULTS

A. Adsorption of C_2H_6

Exposure of the Ru(001) crystal at ∿ 80 K to a beam of C_2H_6 resulted in weak, non-dissociative adsorption. Using TPD at a heating rate of 12 K/s, only one peak was seen in the thermal desorption spectra for increasing C_2H_6 coverage.

The maximum in the desorption rate was at ∿ 91 K and the peak maximum was invariant with coverage, consistent with first order desorption. Assuming a first order pre-exponential of 10^{13}/s, the desorption energy E_d is computed to be 5.0 kcal/mole.[10] Increasing the beam flux did not result in the formation of C_2H_6 multilayers, so that saturation coverage is assumed to be $\lesssim$ 1 monolayer.

The only LEED pattern detected was the (1 x 1) pattern characteristic of the clean substrate; no extra spots due to C_2H_6 adsorption were detected.

The only ESDIAD pattern seen for adsorbed C_2H_6 arose from desorption of a low yield of H^+ ions normal to the surface; no evidence for "lobes" or "halos" were seen in the ESDIAD patterns. Presumably C_2H_6 adsorbs into a disordered mobile layer at ∿ 80 K, with no evidence for either long range translational order or azimuthal order seen in LEED or ESDIAD respectively. Firment and Somorjai[11] have noted that C_2H_6 also does not adsorb in an ordered fashion on Pt(111) at T > 90 K.

B. Adsorption of Cyclopropane, C_3H_6

Cyclopropane is a cycloparaffin with a planar, triangular carbon skeleton having 2 H atoms bonded to each C atom, one on either side of the skeletal plane. Adsorption is weak and non-dissociative, with / indicating thermal desorption measurements rapid desorption at ∿ 145 K. No ordered LEED pattern other than the (1 x 1) pattern characteristic of the clean substrate was seen. ESDIAD studies revealed a broad cone of H^+ emission (fwhm > 30°) symmetric about the normal to the crystal surface. As in the case of C_2H_6, C_3H_6 appears to adsorb into a disordered, mobile layer which does not result in either long range translational or azimuthal order capable of detection using LEED or ESDIAD respectively. LEED studies[11] of propane on Pt(111) have also indicated the absence of two dimensional order at T > 90 K.

C. Adsorption of Cyclohexane, C_6H_{12}

a. Temperature Programmed Desorption of C_6H_{12}

Cyclohexane has a skeleton containing 6 carbon atoms; isomeric forms include the familiar "chair" and "boat" forms shown in Fig. 1. The chair

form, shown in the upper left of Fig. 1, is energetically more stable in the gas phase.

Fig. 2 shows a series of thermal desorption spectra associated with different coverages of C_6H_{12} on Ru(001). The sample was dosed by rotating to face the doser; TPD was accomplished by rotating the crystal so that the crystal normal was approximately coincident with the axis of the QMS. With the QMS tuned to a major C_6H_{12} ion peak, TPD shows that at low coverages, only a single C_6H_{12} binding state having maximum desorption rate at T_p = 227 K is seen. As the C_6H_{12} dosage increases, the coverage in this state increases, but T_p remains nearly constant at 227 K, indicative of first order desorption kinetics. Assuming a pre-exponential of $10^{13}s^{-1}$, the activation energy for first order kinetics is 14.2 kcal/mole.

After saturation of the state at 227 K, further exposure of the crystal to C_6H_{12} leads to the formation of a desorption state (150-175 K) which exhibits no evidence for saturation, but which grows indefinitely with increasing exposure to gaseous C_6H_{12}. Furthermore, the state desorbs following zero order kinetics, i.e., with a desorption rate independent of coverage:

$$\frac{d\sigma}{dt} = \sigma^{\circ}\, \nu e^{-E_d/RT}$$

This is evidenced by the exponential dependence on $\frac{1}{T}$ of intensity (desorption rate) for the leading edge of the desorption peak as demonstrated in Fig. 3. Such kinetics are characteristic of free sublimation from a solid or liquid, and this observation suggests that the state at 150 - 175 K is due to a condensed multilayer of C_6H_{12}. In Fig. 3, we plot the logarithm of the desorption rate, taken from the leading edge of a TPD spectrum similar to the top curve of Fig. 2, vs. 1/T. The slope of this curve yields a desorption energy of 9.2 kcal/mole, in good agreement with the heat of sublimation of solid C_6H_{12}, 9.0 kcal/mole.[12] Thus, a kinetic

method (TPD) yields data in good agreement with equilibrium thermodynamics. For comparison, Fig. 3 also shows similar data for TPD of an H_2O ice multilayer in which the desorption energy of 11.5 kcal/mole agrees well with the heat of sublimation of amorphous ice, estimated to be 12.2 kcal/mole.[13] Fig. 2 also demonstrates another characteristic of zero order TPD from multilayers: when the multilayer is exhausted, the desorption rate drops precipitously to a low value.

We conclude that the C_6H_{12} desorbing in the peak at 227 K is due to C_6H_{12} adsorbed in the <u>first monolayer</u> in contact with the Ru(001) substrate; the monolayer peak reaches saturation before the multilayer forms. The fact that T_p for C_6H_{12} is higher than those of C_2H_6 and C_3H_6 suggests that the C_6H_{12} is adsorbed in a configuration in which a large fraction of the C atoms are close to the substrate, viz., a more or less "lying down" mode.

In closing this discussion of TPD of C_6H_{12}, we note that structure has also been seen in the TPD spectra in the range 150 - 175 K, and is believed to be due to the formation of the <u>first</u> condensed layer adsorbed <u>on top of the monolayer</u>. This feature is not shown in the TPD spectra of Fig. 2, but a similar feature can be seen in the TPD spectra of Fig. 10, discussed below in Section III D. This layer appears to have a slightly higher desorption energy ($\sim$ .2 kcal/mole) than the remainder of the condensed multilayer at higher coverages. Another general observation is that a small amount of H_2 is observed to desorb at 350 - 500 K following C_6H_{12} desorption. This signal may be due to residual background H_2 adsorption, or to decomposition of a small fraction of the C_6H_{12}.

Thus, C_6H_{12} is adsorbed primarily as a molecular species on Ru(001) at 80 K, and the TPD studies provide a clear indication of the various adsorption regimes.

b. ESD of C_6H_{12}

In this section, we will discuss the ESD behavior of C_6H_{12} on Ru(001) as characterized using the QMS detector. The discussion of the LEED and ESDIAD results follows in Section III.C.c.

The ESD of C_6H_{12} at coverages $\lesssim$ 1 monolayer results in the desorption of H^+ ions (V_e = 150 eV, $J_e = 2 \times 10^{-5} A/cm^2$); no other ionic species were detected using the QMS. The total desorption cross section determined from the decay of H^+ ion current as a function of time is $(8 \pm 2) \times 10^{-17}$ cm^2 and is comparable to typical gas phase dissociative ionization cross sections.

An H^+ ESD signal is also observed for multilayer C_6H_{12} adsorption. Fig. 4 is a plot of H^+ signal intensity as a function of the temperature to which the sample had been heated for $\sim$ 1 sec, following adsorption of a C_6H_{12} multilayer. Note that on this logarithmic plot, the H^+ signal drops precipitously during desorption of the multilayer and monolayer, and that a small residual H^+ signal due to H_2 impurities and/or slight C_6H_{12} decomposition is seen at higher temperatures.

ESD of a C_6H_{12} multilayer yields a host of ionic desorption products in addition to H^+. Fig. 5a shows the observed QMS cracking pattern for gas phase C_6H_{12}, and Fig. 5b illustrates the QMS signal for ESD products from a C_6H_{12} multilayer. In order to enhance sensitivity, the resolution of the QMS has been reduced below that required to give unit mass resolution, so that only envelopes of closely lying mass peaks are seen. Virtually the entire gas phase cracking pattern is seen in ESD, although with varying intensities. Thus, the ESD of a C_6H_{12} monolayer yields <u>only</u> H^+, whereas the multilayer yields many more ionic fragments (Fig. 6); in addition, the H^+ ion yield from the multilayer is much greater than that of the monolayer (Fig. 4).

These observations are supportive of the ESD mechanism originally formulated by Redhead[14] and Menzel and Gomer.[15] The monolayer species are in intimate contact with the substrate. The probability for electronic excitation to a repulsive or ionic state is high, but de-excitation processes involving electron tunneling from the substrate are also highly probable, so that the net ion flux

from the adsorbed layer is low. In addition, the probability of desorption of slower moving, more massive ion fragments is suppressed due to the ESD isotope effect.[16] Hence, the dominant ionic desorption fragment is H^+. Note, however, that the total cross section[16] (Fig. 7) for destruction of the multilayer species giving rise to the H^+ signal is high, $\sim 8 \times 10^{-17} cm^2$, and is comparable to gas phase total ionization cross sections.[17]

In an insulating multilayer, deexcitation processes involving electron tunneling from the substrate are virtually non-existent, although intramolecular collisional deactivation cannot be eliminated. The observation of higher mass ionic fragments is a consequence of the availability of repulsive ionic states for Franck-Condon excitation as well as the reduced deexcitation probability in the multilayer. Note, however, that the higher mass ESD fragments in Fig. 5b are attenuated by comparison with the gas phase mass spectrum. If we assume that this attenuation is a simple consequence of the ESD mass effect[16] (in which slower-moving heavy ions are more effectively neutralized than faster-moving light ions), then we can estimate the expected magnitude of the attenuation. By assuming an escape probability of 0.1 for the mass 27 ions, the intensities given by the dashed lines in Fig. 5b are computed using the formalism of Ref. 16 (i.e., the higher mass fragments in the gas phase cracking pattern are attenuated relative to mass 27). Although the intensity at mass 41 is not accurately predicted by this model, the higher mass intensities are in reasonable agreement with experiment. However, the possibility of an experimental artifact (energy dependence of QMS transmission) being partly responsible for the high mass attenuation has not been eliminated.

Fig. 7 shows a series of data illustrating the decay of intensity of several ionic fragments as a function of electron bombardment time for a C_6H_{12} multilayer. In all cases, the total cross sections for depletion of the species giving rise to the ions is quite high, $2 - 10 \times 10^{-17} cm^2$. Even at a beam current as low as $1.2 \times 10^{-7} A$ ($J \sim 1.5 \times 10^{-5} A/cm^2$) the lifetime of the adsorbed layer is of the order of 100 seconds. This places a severe limitation on measurement times using electron beams for the study of hydrocarbon layers as in LEED and AES.

c. ESDIAD and LEED Studies of C_6H_{12}

Fig. 8 shows LEED and ESDIAD patterns associated with C_6H_{12} on Ru(001). Fig. 8a is the LEED pattern associated with the clean hexagonally-symmetric Ru(001) surface. Upon adsorption of fractional monolayers of C_6H_{12} on this surface at $\sim$ 80 K, no "extra" LEED beams were seen (V_e = 90 - 200 eV); the only pattern visible was the (1 x 1) pattern characteristic of the clean surface. Either the adlayer is disordered, or it orders into the (1 x 1) structure of the substrate. Such ordering appears impossible, however, since the molecular diameter of C_6H_{12} is greater than the Ru-Ru spacing, and severe compression of the adlayer would be required. In contrast, Firment and Somorjai[11] report ordered overlayers of monolayer coverages of cyclohexane on Pt(111) at 140 - 200 K; the C_6H_{12} molecules are out-of-registry with the underlying Pt atoms in their model.

Fig. 8c is the ESDIAD pattern associated with fractional monolayers of C_6H_{12}. The pattern is characterized by a bright spot in the center due to an ion beam emitted normal to the surface, and 6 very faint lobes of emission arranged symmetrically about the center spot. Because of the difficulty in photographically reproducing the faint lobes in Fig. 8c, we show a sketch of this pattern in Fig. 8e to indicate the relative sizes and orientations of the lobes. Note that the expected symmetry in Fig. 8a and 8c is hexagonal, although the resultant LEED and ESDIAD patterns are not perfect hexagons. This is a result of distortion of the charged particle trajectories by the electric field between the irregularly shaped sample and the first hemispherical grid). As discussed previously, the only ESD ion detected from the C_6H_{12} monolayer is H^+.

The ESDIAD pattern (8c,8e) and the LEED pattern (8a) have the same azimuthal registry. However, the LEED pattern has the orientation of the reciprocal lattice net, and is rotated by 30° with respect to the substrate atom net. In contrast, the ESDIAD pattern is a view in direct space of the

desorbing ion trajectories.

The symmetry of the ESDIAD pattern 8c is consistent with the symmetry of the C_6H_{12} molecule, and a model for adsorption on the Ru(001) surface will be discussed in Section IV, below. We simply note here that the size of the carbon skeleton of C_6H_{12} is such as to fit nicely on a single Ru atom. If such is the case, then Fig. 8c suggests that the mean azimuthal orientation of the CH bonds in adsorbed C_6H_{12} is in the direction of next-nearest neighbor surface atoms (in contrast, the OH bonds in adsorbed H_2O are in the direction of nearest neighbors).[8]

Fig. 8b is a LEED pattern associated with a multilayer of C_6H_{12} adsorbed at 80 K. This pattern is quite dim, and is very susceptible to ESD damage. Electron bombardment at 200 eV, 1.5×10^{-7}A for $\sim$ 20s to 30s is sufficient to cause the extra features to disappear. The pattern is complex and has not been analyzed; it is shown merely to illustrate that multilayer C_6H_{12} films are apparently crystalline and to confirm that ESD effects do seriously effect the LEED pattern. The lifetime of the LEED pattern for multilayer C_6H_{12} is consistent with ESD cross sections as well as with previous observations.[11]

Fig. 8d is an ESDIAD pattern from multilayer C_6H_{12}. The bright spot is due to emission normal to the surface, and contains contributions from H^+ through $C_6H_{12}^+$. The angular size of the H^+ contribution to this beam is displayed in Fig. 9 as a plot of QMS H^+ signal as a function of ion desorption angle. Similar data for higher mass fragments exhibited similarly wide (fwhm > 30°) ion angular distributions. (Note that the data of Fig. 9 were obtained using a bias potential V_B = 40V between the sample and the QMS entrance aperture. The resultant electric field causes a decrease in the width of the ESDIAD beams;[18] the zero field width of the H^+ cone from C_6H_{12} is certainly greater than the 30° shown here.)

In summary, it appears that fractional monolayers of C_6H_{12} are adsorbed at $\sim$ 80 K in a layer in which long range order is absent. Most importantly the orientation of the ESDIAD pattern contains information regarding the mean azimuthal orientation of the CH bonds.

D. Adsorption of Cyclooctane, C_8H_{16}

Cyclooctane is a saturated cycloparaffin with a "puckered" ring carbon skeleton. Exposure of the Ru(001) crystal at 80 K to a beam of C_8H_{16} results first in population of a "monolayer" state of C_8H_{16} in direct contact with the substrate. Temperature programmed desorption studies (Fig. 10) demonstrate that T_p for this state is $\sim$ 270 K when $\theta \sim 0.1$; decreasing to $\sim$ 257 K for $\theta \sim 1.0$. (N.B. For each curve in Fig. 10, the precision of the temperature scale is $\pm$ 3° at $\sim$ 250 K; the accuracy is estimated at $\pm$ 10 K). Upon saturation of the monolayer, subsequent C_8H_{16} adsorption leads to the population of a second layer of physisorbed molecules. Further adsorption results in population of a multilayer state which desorbs following zero order kinetics, as observed previously for H_2O and C_6H_{12} multilayers.

The activation energy for desorption of C_8H_{16} from the monolayer state decreases slightly as a function of coverage due to intramolecular interactions; at $\theta = 1$, $T_p = 257$ K, the first order activation energy, computed assuming a preexponential factor of $10^{13}sec^{-1}$, is 16.2 kcal/mole.

The ESD results for C_8H_{16} parallel those for C_6H_{12}. ESD of fractional monolayers of C_8H_{16} yields H^+ as the only ionic desorption product, whereas ESD of C_8H_{16} multilayers yields a spectrum of ionic fragments qualitatively similar to the gas phase cracking pattern. As in the case of C_6H_{12}, the higher mass fragments are attenuated more than the corresponding species in the gas phase cracking pattern, fr the reasons discussed in III.C.b.

Adsorption of fractional monolayers of C_8H_{16} results in no new LEED structures other than the familiar (1 x 1). For fractional monolayer doses, the ESDIAD pattern has a mottled, somewhat textured appearance with no regular symmetry apparent. As discussed in Section IV below, it appears most reasonable that the C_8H_{16} molecule is bonded to the substrate with the carbon skeleton generally

parallel to the substrate. There is no regular azimuthal registry with the substrate.

IV. DISCUSSION

A. Bonding Characteristics of C_2H_6 and Cycloparaffins Adsorbed on Ru(001).

For all of the molecules studied (C_2H_6,C_3H_6,C_6H_{12},C_8H_{16}), the temperature programmed desorption (TPD) data indicate that adsorption on Ru(001) is non-dissociative at $\sim$ 80 K. Following formation of a surface monolayer, the larger molecules (C_6H_{12} and C_8H_{16}) form condensed multilayers whose desorption characteristics are consistent with free sublimation from solid hydrocarbon layers. For both C_6H_{12} and C_8H_{16}, there is also evidence for the formation of a second layer with binding energy between that of the first monolayer and the condensed multilayer. Thus, the effect of the substrate extends in a weak fashion into the second layer, but is absent for higher coverages.

Fig. 11 illustrates the TPD characteristics of monolayer quantities of the hydrocarbon molecules on Ru(001). Fig. 11a is a plot of T_p, the temperature at which the desorption rate is a maximum (cf. Figs. 2 and 10), as a function of the number of carbon atoms in each molecule. Assuming first order desorption kinetics and a pre-exponential factor of $10^{13}s^{-1}$, these values of T_p were used to compute[10] activation energies for desorption, E_d. The resultant values of E_d are plotted vs. the number of carbon atoms in each molecule in Fig. 11b. The monotonic increases seen in both 11a and 11b suggest that the molecules are bonded to the Ru(001) substrate in such a way as to maximize coordination with the substrate. That is, the carbon skeletons of each molecule are oriented more-or-less parallel to the Ru surface. If "edge-on" bonding through only one or two methylene groups were to occur for the larger ring structures, the measured values of E_d would be lower, comparable to the C_2H_6 or C_3H_6 data. Moreover, the magnitudes of E_d are only slightly higher than the heats of sublimation of the molecular solids,

suggesting that physical adsorption or very weak chemisorption occurs, and that the geometric and electronic structures of the gas phase molecules are relatively unperturbed in the adsorbed layer.

Although adsorption of the cycloparaffins is non-dissociative on Ru(001) at low temperatures, dissociative adsorption of C_6H_{12} on Pt and Ir surfaces has been observed to occur at T > 300 K.[19] Demuth, Ibach and Lehwald[20] have reported that cyclohexane reversibly desorbs from Ni(111) for $T \gtrsim 170$ K, but dehydrogenates on Pt(111) for $T \geq 200$ K to leave benzene.

The absence of structured ESDIAD patterns for ethane and cyclopropane is consistent with the lack of long-range order observed using LEED, and suggests that these species are adsorbed into disordered, possibly mobile layers in which short-range azimuthal registry with the substrate is also absent. The C_8H_{16} molecule is apparently too large and"puckered" to form a layer having either short or long range order, so that no ordered LEED or ESDIAD patterns are seen. Cyclohexane does yield a hexagonal ESDIAD pattern (Fig. 8c), and the following adsorption model is proposed.

The conformation of cyclohexane[21] has been well studied in the liquid phase as a function of temperature using NMR techniques.[22] The thermodynamically stable form of C_6H_{12} is the chair form (Fig. 1) which is 5.3 ± 0.3 kcal/mole more stable than the boat form.[23] Jensen, et al. have used NMR to measure the temperature dependence of the rate of inversion of chair form C_6H_{12} (which proceeds via strained conformation) and they deduce that $\Delta H^* = 9.7$ kcal/mole. At 77 K the rate for inversion is negligibly small.[22] Thus it is reasonable to consider that in the absence of strong perturbations due to adsorption of C_6H_{12} by Ru(001), we are dealing essentially with stable chair form - C_6H_{12} in the adsorbed layer.

In Figure 12 is shown a model of chair form-C_6H_{12}, and its probable steric relationship to a Ru(001) site. The hydrogens in C_6H_{12} are divided into

two general groups, designated axial and equatorial. The axial hydrogens are directed up and down from the carbon skeleton ring and are shown by open circles and starred circles. The six equatorial hydrogens are designated by open circles and black circles with the black circles representing those hydrogens directed slightly upwards from the plane. In the lower portion of the figure the projection of the starred axial hydrogens onto the Ru(001) site is shown and an excellent fit into three equivalent wells in the Ru(001) surface is seen to occur. When the chair form-C_6H_{12} is so oriented three of the axial hydrogens (dark circles) are directed through the valleys between neighboring Ru atoms, as shown in the lower portion of the figure. ESDIAD from this molecule would yield the non-normal H^+ -ejection directions which are experimentally observed, i.e., in the direction of <u>next-nearest</u> Ru neighbors relative to the central Ru atom. Six equivalent ejection directions would result from two equivalent orientations of C_6H_{12}, rotated 60° with respect to each other. In addition, ESDIAD on this molecule would be expected to yield a <u>normal</u> H^+ beam from the upward pointing axial hydrogens, and this normal H^+ emission is also experimentally observed from monolayer C_6H_{12} on Ru(001). It is not possible at present to answer two questions of importance to a complete interpretation of ESDIAD results for C_6H_{12} on Ru(001):

(a) Are the two types of equatorial hydrogens distinguishable? Do the downward directed equatorial hydrogens (open circles) contribute to the hexagonal H^+ beams?

(b) What is the observed polar angle of emission of the hexagonal H^+ beams, and what factors are at work in determining the polar angle direction of emission of these beams (i.e. distortion of bond angle in weakly-held adsorbed species, image force attractive perturbations of initial H^+ trajectory, possible repulsive forces from Ru atoms on H^+ trajectory, etc.)?

B. Electron Beam-Induced Damage in Hydrogen Layers

In the present studies, ESD effects in adsorbed hydrocarbon layers were monitored by detection of ionic desorption products and by changes in the appearance of the LEED pattern (in the case of multilayer C_6H_{12}). For monolayer and fractional monolayer coverages, the only ionic desorption product seen from any of the adsorbed hydrocarbons is H^+. In all of these cases, the total cross section for depletion of the species giving rise to the H^+ signal is $\sim 10^{-16} cm^2$, comparable to gas phase dissociative ionization cross sections.[17] Presumably, excitation of more massive ionic fragments to repulsive electronic states does not occur, and/or the desorption probability of heavier ionic fragments is very low due to effective neutralization processes[7] ("bond healing" effects due to electron transfer from the metallic substrate).

On the contrary, ESD of multilayers results in the appearance of a host of ionic fragments having distributions similar to gas phase mass spectrometer cracking patterns. There is an attenuation in the intensity of the heavier fragments consistent with intermolecular deactivation processes in the condensed multilayer. The condensed multilayers are sufficiently removed from the metallic substrate ($\gtrsim 5$ Å) so that neutralization processes involving electron transfer (Auger neutralization, resonance tunneling, etc.) from the substrate are not likely.

These data are consistent with the LEED studies of Buchholz and Somorjai[24] and Firment and Somorjai.[11] They demonstrated that the disappearance time for the C_6H_{12} multilayer LEED pattern was $\sim$ 5s at a current density of $5 \times 10^{-5} A/cm^2$; the present results indicate a disappearance time of 20 to 30s at $1.5 \times 10^{-5} A/cm^2$. They also noted that surfaces of solids composed of large conjugated aromatic molecules are more stable under electron beam irradiation than surfaces of smaller conjugated molecules, and that surfaces of saturated molecules are even less stable.

Finally, there is ample evidence to indicate that electron bombardment of hydrocarbon layers can lead to many complex chemical effects in addition to ionic desorption. Matsuhige and Hamill[25] have seen evidence for radical-radical interactions leading to desorption of bicyclohexyl ($(C_6H_5)_2$) during low energy electron bombardment of cyclohexane. Electron bombardment of surface layers can also result in polymerization; electron-beam polymerization finds wide use in the fabrication of microelectronic circuits.[26]

In conclusion, we have demonstrated that a combination of surface sensitive methods (LEED, ESD and ESDIAD) provides new insights into the structure and bonding of hydrocarbons adsorbed on metals.

V. ACKNOWLEDGEMENT

This work was supported in part by the Office of Naval Research.

REFERENCES

(1) J. B. Pendry, "Low Energy Electron Diffraction: The Theory and its Application in Determination of Surface Structure", (Academic Press, NY, 1974).

(2) M. A. Van Hove and S. Y. Tong, Phys. Rev. Lett. 35, 1092 (1975).

(3) L. L. Kesmodel, P. C. Stair, R. C. Baetzold and G. A. Somorjai, Phys. Rev. Lett. 36 1316 (1976).

(4) E. W. Plummer, Proc. 7th Intern. Vac. Congr. and 3rd Intern. Conf. Solid Surfaces, Vienna 1977 (Ed. and Publ., R. Dobrozemsky, et. al.), p. 647.

(5) C. L. Allyn, T. Gustafsson and E. W. Plummer, Chem. Phys. Lett. 47, 127 (1977).

(6) T. E. Madey, J. J. Czyzewski, and J. T. Yates, Jr., Surface Science 49, 465 (1975).

(7) T. E. Madey and J. T. Yates, Jr., Surface Science 63, 203 (1977).

(8) T. E. Madey and J. T. Yates, Jr., Chem. Phys. Lett. 51, 77 (1977); also, Proc. 7th Intern. Vac. Congr. and 3rd Intern. Conf. Solid Surfaces, Vienna 1977 (Ed. and Publ., R. Dobrozemsky, et. al.) p. 1183.

(9) T. E. Madey, H. A. Engelhardt, and D. Menzel, Surface Sci. 48, 304 (1975).

(10) P. A. Redhead, Vacuum 12, 203 (1962).

(11) L. E. Firment and G. A. Somorjai, J. Chem. Phys., 66, 2901 (1977).

(12) Computed from vapor pressure data in Handbook of Chemistry and Physics, Chem. Rubber Co.

(13) N. H. Fletcher, "The Chemical Physics of Ice" (Cambridge Univ. Press, 1970).

(14) P. A. Redhead, Can. J. Phys. 42, 886 (1964).

(15) D. Menzel and R. Gomer, J. Chem. Phys. 41, 3311 (1964).

(16) T. Madey and J. T. Yates, Jr., J. Vac. Sci. Technol. 8, 525 (1971); T. E. Madey, J. T. Yates, Jr., D. A. King and C. J. Uhlaner, J. Chem. Phys. 52, 5215 (1970); C. Leung, Ch. Steinbruchel and R. Gomer, Appl. Phys. 14, 79 (1977).

(17) J. W. Otvos and D. P. Stevenson, J. Am. Chem. Soc. 78, 546 (1956); D. Rapp and P. Englander-Golden, J. Chem. Phys. 43, 1464 (1965).

(18) T. E. Madey, to be published.

(19) B. E. Niewenhuys, D. I. Hagen, G. Rovida and G. A. Somorjai, Surface Sci. 59, 155 (1976); K. Baron, D. W. Blakeley, and G. A. Somorjai, Surface Sci. 41, 45 (1974).

(20) J. E. Demuth, H. Ibach, and S. Lehwald, Phys. Rev. Letters, to be published.

(21) See M. S. Newman, "Steric Effects in Organic Chemistry", p. 13, J. Wiley and Sons, Inc., New York (1956).

(22) F. R. Jensen, D. S. Noyce, C. H. Sederholm, and A. J. Berlin, J. Amer. Chem. Soc., 82, 1256 (1960).

(23) W. S. Johnson, J. L. Margrave, V. J. Bauer, M. A. Frisch, L. H. Dreger, and W. M. Hubbard, J. Amer. Chem. Soc., 82, 1255 (1960).

(24) J. C. Buchholz and G. A. Somorjai, J. Chem. Phys. 66, 573 (1977).

(25) T. Matsuhige and W. H. Hamill, J. Phys. Chem. 76, 1255 (1972).

(26) J. J. Licari, "Plastic Coatings for Electronics", (McGraw-Hill Book Co., 1970) p. 186.

FIGURE CAPTIONS

Fig. 1. Carbon skeletons for gaseous cyclohexane, C_6H_{12}. The "chair" form, left, is thermodynamically more stable than the "boat" form, right.

Fig. 2. Temperature programmed desorption spectra following the adsorption of C_6H_{12} on Ru(001) at ∿ 80 K. The heating rate is ∿ 20 K/s.

Fig. 3. Plots of desorption rate vs. 1/T for desorption from multilayers of H_2O and C_6H_{12} adsorbed on Ru(001). The activation energies given by the slopes of the lines are very close to the heats of sublimation of the solids.

Fig. 4. Decay of H^+ ESD ion current as a function of sample temperature during desorption of C_6H_{12} from Ru(001). Multilayer C_6H_{12} was adsorbed at ∿ 80 K, and the sample was heated in steps to the indicated temperature for ∿ 1s.

Fig. 5. Comparison of gas phase mass cracking pattern for C_6H_{12} (a) with the ionic ESD products from multilayer C_6H_{12} (b). The resolution of QMS was the same in each case. Electron energy for gas phase = 70 eV; electron energy for ESD = 200 eV; ionkinetic energy at QMS = 100 eV.

Fig. 6. Schematic illustration of the nature of the ionic ESD products from monolayer and multilayer C_6H_{12}.

Fig. 7. Time dependence of the ESD ion signals from a C_6H_{12} multilayer during electron bombardment (I_e = 1.2 x 10^{-7}A, V_e = 150 eV). Cross sections are determined from the initial slopes as described in Ref. 16.

Fig. 8. LEED and ESDIAD patterns for C_6H_{12} on Ru(001).

(a) clean LEED pattern, V_e = 210 V.

(b) LEED pattern from C_6H_{12} multilayer, Ve = 170 V . The dark "blotches" are due to defects in the imaging system.

(c) ESDIAD pattern from a fractional monolayer of C_6H_{12} on Ru(001) at ∿ 80 K. Note the symmetry and registry of this pattern in comparison with the LEED pattern (a). V_e = 200 V.

(d) ESDIAD pattern from multilayer C_6H_{12}. V_e = 200 V.

(e) Schematic drawing of ESDIAD pattern (c) from fractional monolayer of C_6H_{12} on Ru(001) at ∿ 80 K.

Fig. 9. Angular distribution of H^+ ESD signal from C_6H_{12} multilayer as measured using the QMS ($\sim 5°$ acceptance angle). Application of a bias potential, V_B = 40V, between crystal and QMS detector causes the measured ESDIAD cone angle to be smaller than the true angle (see text).

Fig. 10. Temperature programmed desorption spectra following the adsorption of cyclooctane (C_8H_{16}) on Ru(001) at $\sim$ 80 K. The desorption ranges of the monolayer in contact with the Ru substrate, the second layer and the multilayer are all indicated.

Fig. 11. Variation of Temperature Programmed Desorption behavior of hydrocarbon monolayers on Ru(001) as a function of the number of carbon atoms in each molecule. T_p is the temperature at which the desorption rate is a maximum, and E_d is the activation energy for desorption.

Fig. 12. Model for adsorption of C_6H_{12} on Ru(001) (see text).

Cyclohexane

Fig. 1.

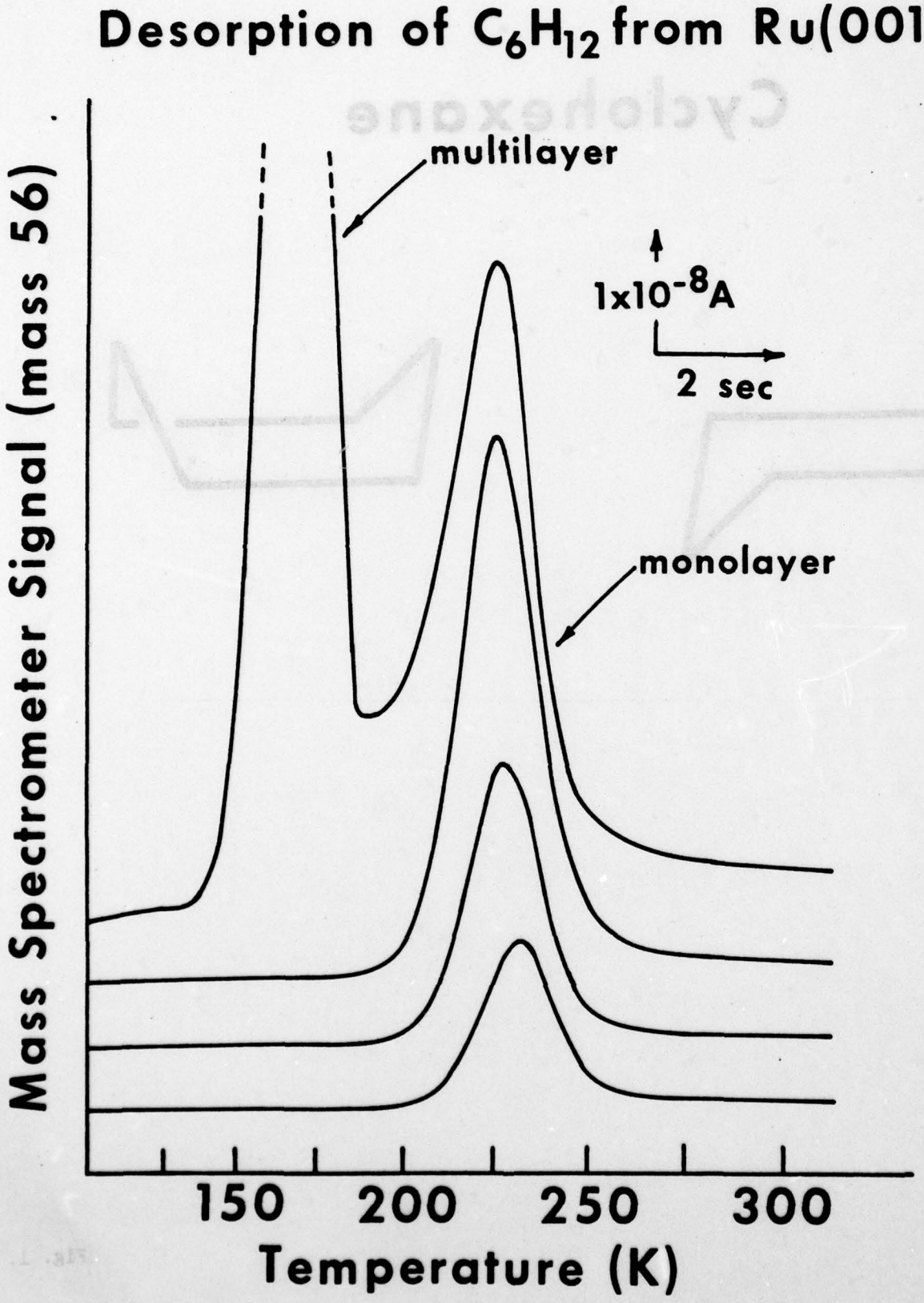
Desorption of C_6H_{12} from Ru(001)
multilayer
$1x10^{-8}$A
2 sec
monolayer
Mass Spectrometer Signal (mass 56)
150
200
250
300
Temperature (K)

Fig. 2.

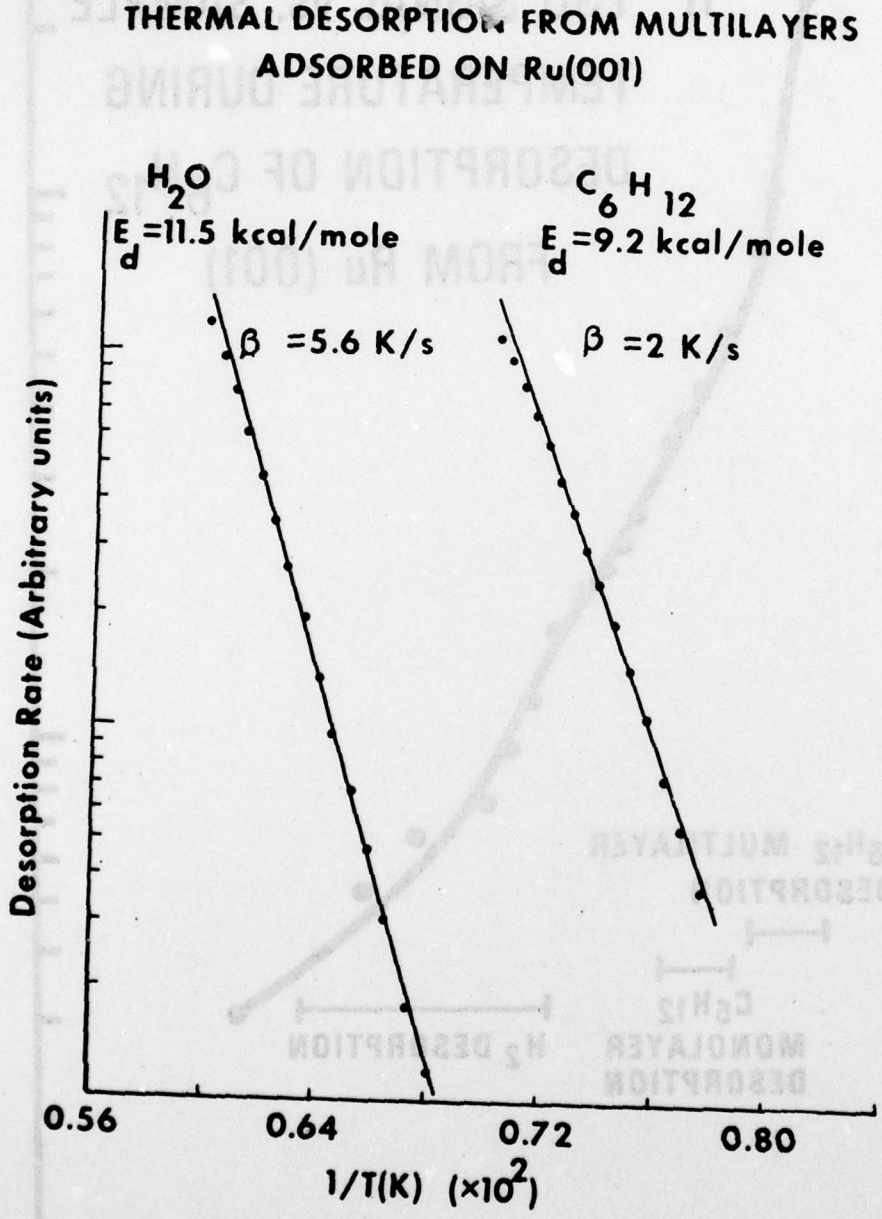
THERMAL DESORPTION FROM MULTILAYERS
ADSORBED ON Ru(001)
H_2O
E_d=11.5 kcal/mole
β =5.6 K/s
C_6H_{12}
E_d=9.2 kcal/mole
β =2 K/s
Desorption Rate (Arbitrary units)
0.56
0.64
0.72
0.80
1/T(K) (×10²)

Fig. 3.

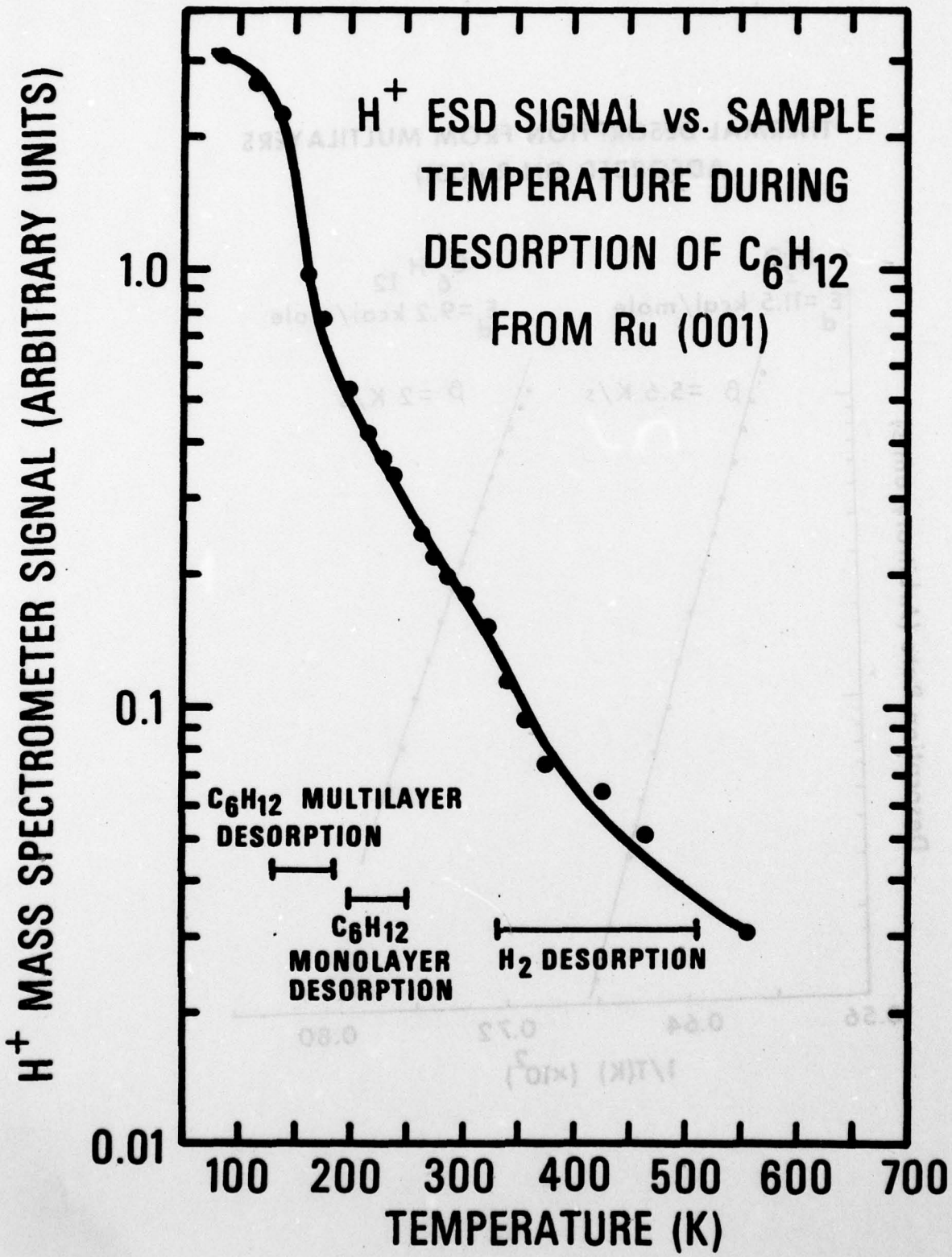
H+ ESD SIGNAL vs. SAMPLE TEMPERATURE DURING DESORPTION OF C6H12 FROM Ru (001)
H+ MASS SPECTROMETER SIGNAL (ARBITRARY UNITS)
1.0
0.1
0.01
C6H12 MULTILAYER DESORPTION
C6H12 MONOLAYER DESORPTION
H2 DESORPTION
100
200
300
400
500
600
700
TEMPERATURE (K)

Fig. 4.

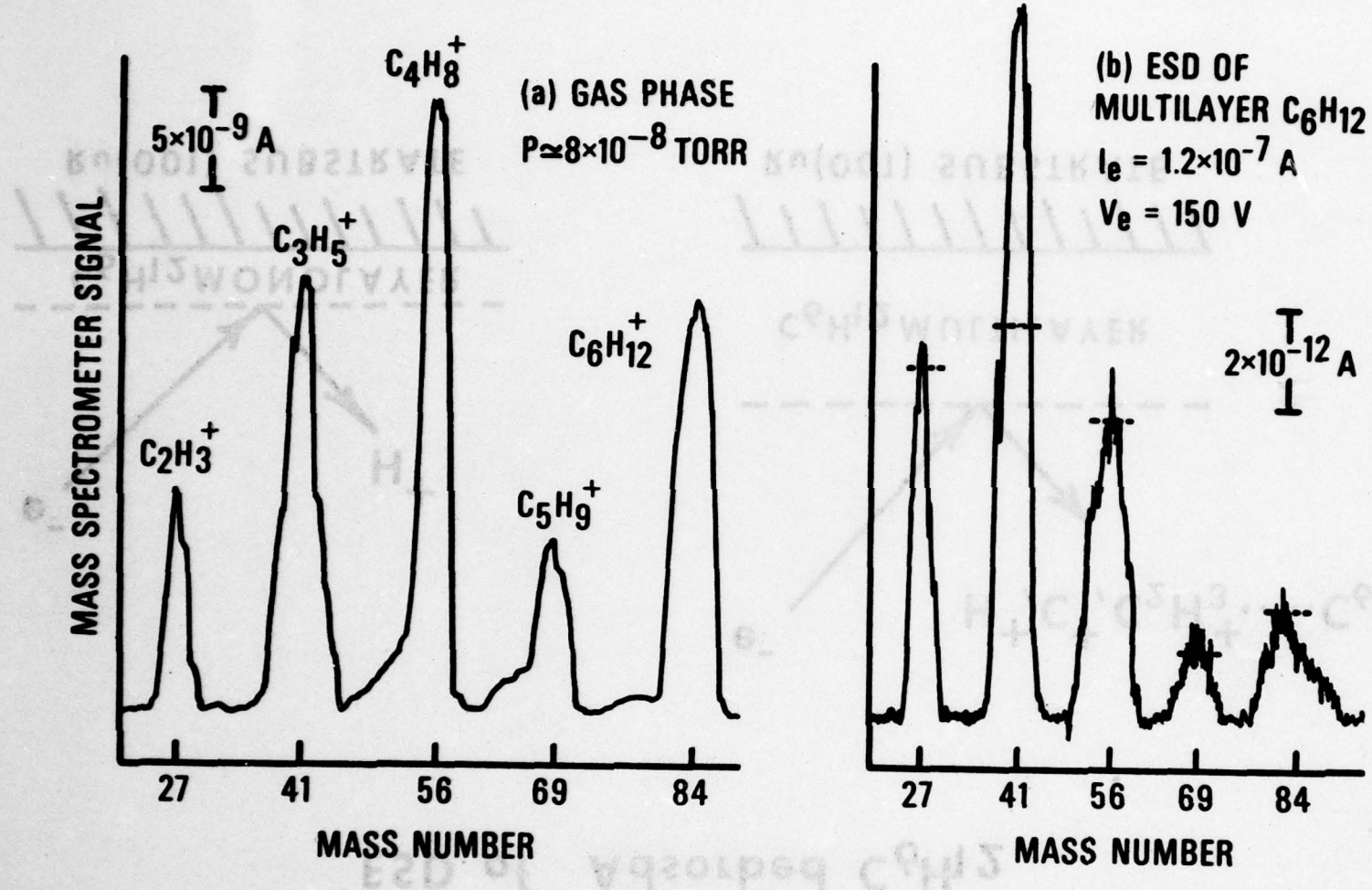
COMPARISON OF GAS PHASE C_6H_{12} CRACKING PATTERN WITH ESD OF C_6H_{12} MULTILAYER
MASS SPECTROMETER SIGNAL
5×10^{-9} A
$C_2H_3^+$
$C_3H_5^+$
$C_4H_8^+$
$C_5H_9^+$
$C_6H_{12}^+$
(a) GAS PHASE
$P\simeq8\times10^{-8}$ TORR
27
41
56
69
84
MASS NUMBER
(b) ESD OF MULTILAYER C_6H_{12}
$I_e = 1.2\times10^{-7}$ A
V_e = 150 V
2×10^{-12} A
27
41
56
69
84
MASS NUMBER

Fig. 5.

ESD of Adsorbed C_6H_{12}

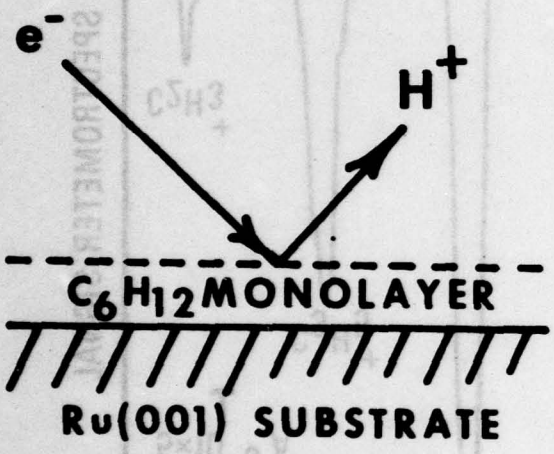

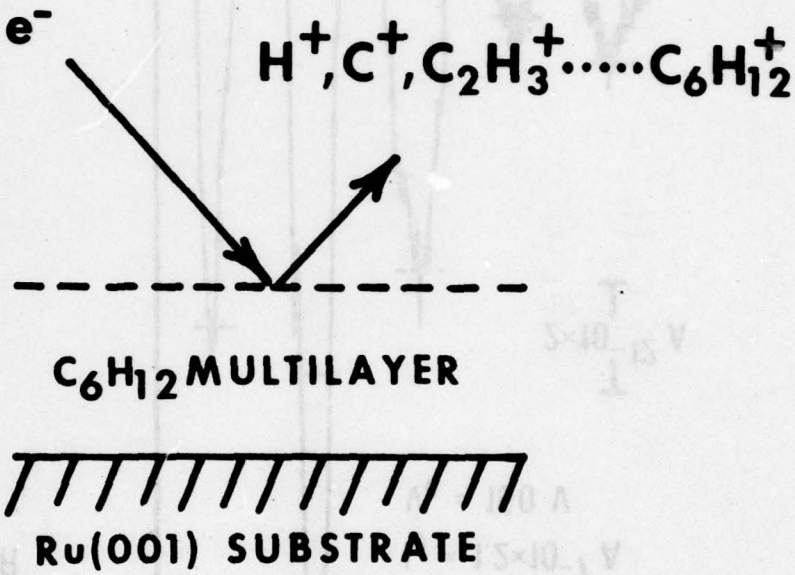

Fig. 6.

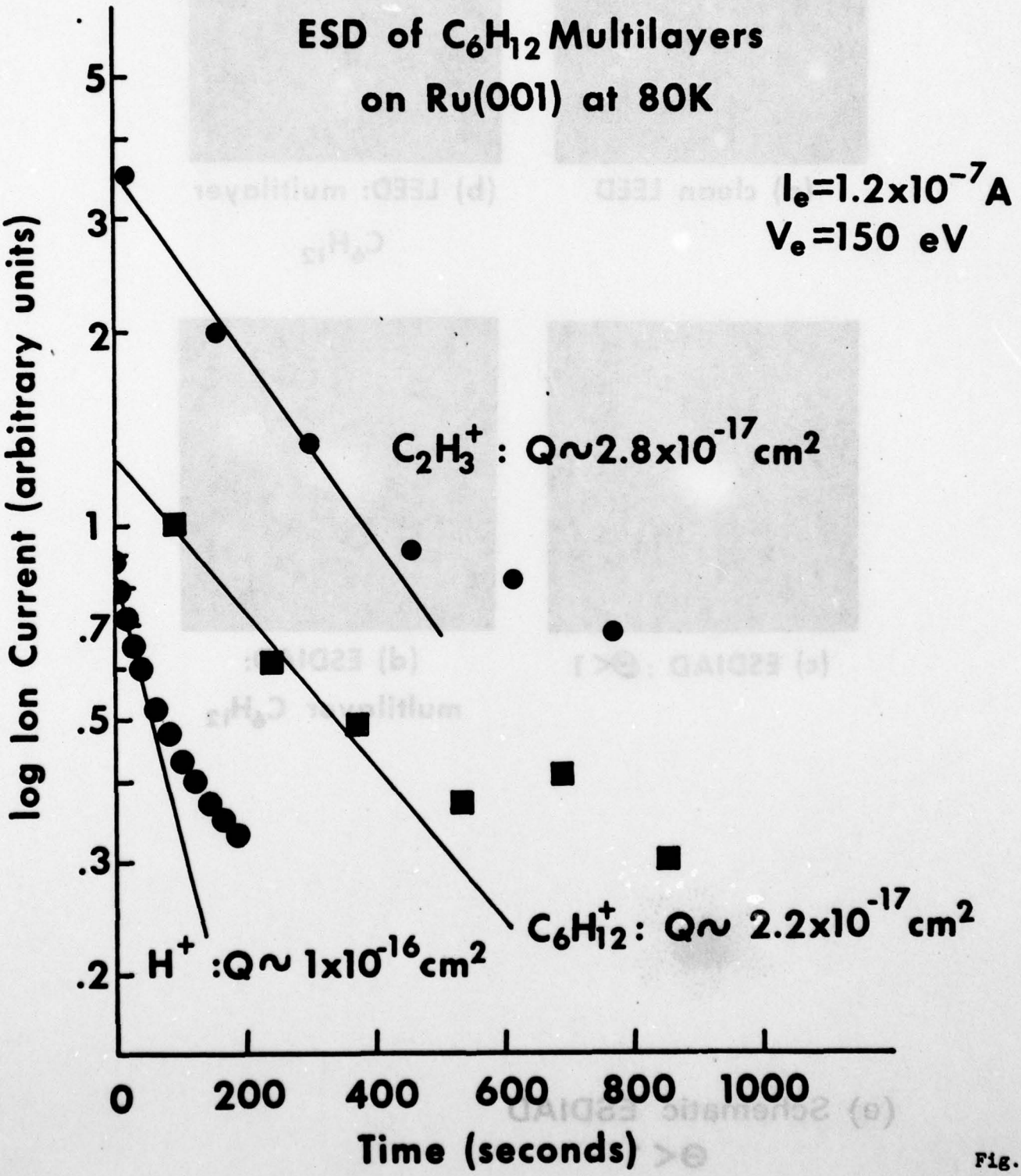
ESD of C_6H_{12} Multilayers
on Ru(001) at 80K
I_e=1.2x10^{-7}A
V_e=150 eV
$C_2H_3^+$: Q~2.8x10^{-17}cm^2
$C_6H_{12}^+$: Q~ 2.2x10^{-17}cm^2
H^+ :Q~ 1x10^{-16}cm^2
log Ion Current (arbitrary units)
5
3
2
1
.7
.5
.3
.2
0
200
400
600
800
1000
Time (seconds)

Fig. 7.

Physical Adsorption of C_6H_{12} on Ru(001)

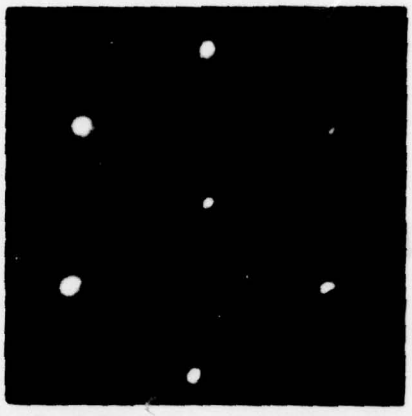

(a) clean LEED

(b) LEED: multilayer C_6H_{12}

(c) ESDIAD : $\Theta < 1$

(d) ESDIAD: multilayer C_6H_{12}

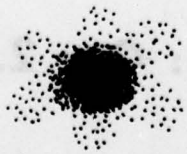

(e) Schematic ESDIAD $\Theta < 1$

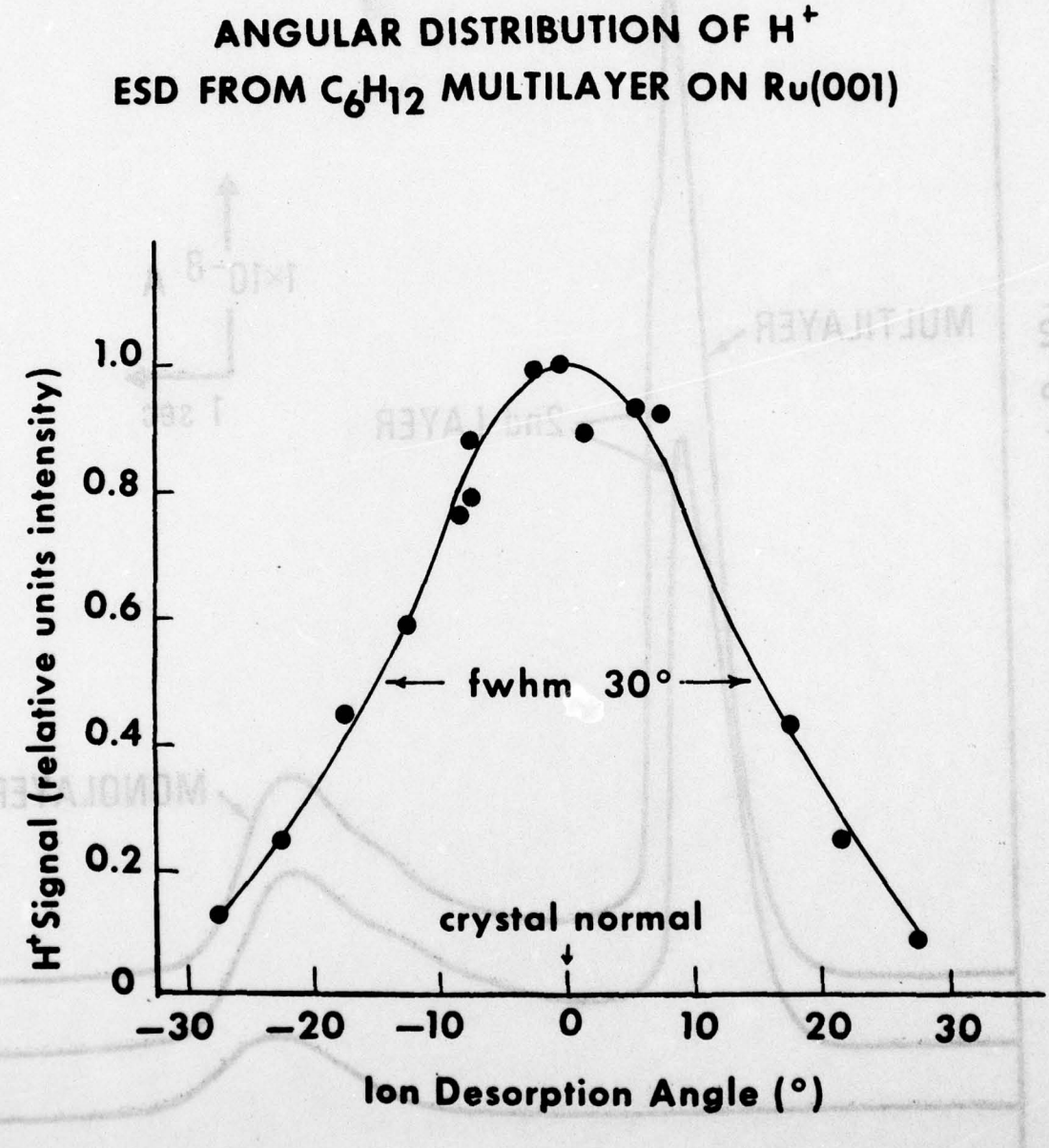
ANGULAR DISTRIBUTION OF H+
ESD FROM C6H12 MULTILAYER ON Ru(001)
H+ Signal (relative units intensity)
1.0
0.8
0.6
0.4
0.2
0
fwhm 30°
crystal normal
−30
−20
−10
0
10
20
30
Ion Desorption Angle (°)

Fig. 9.

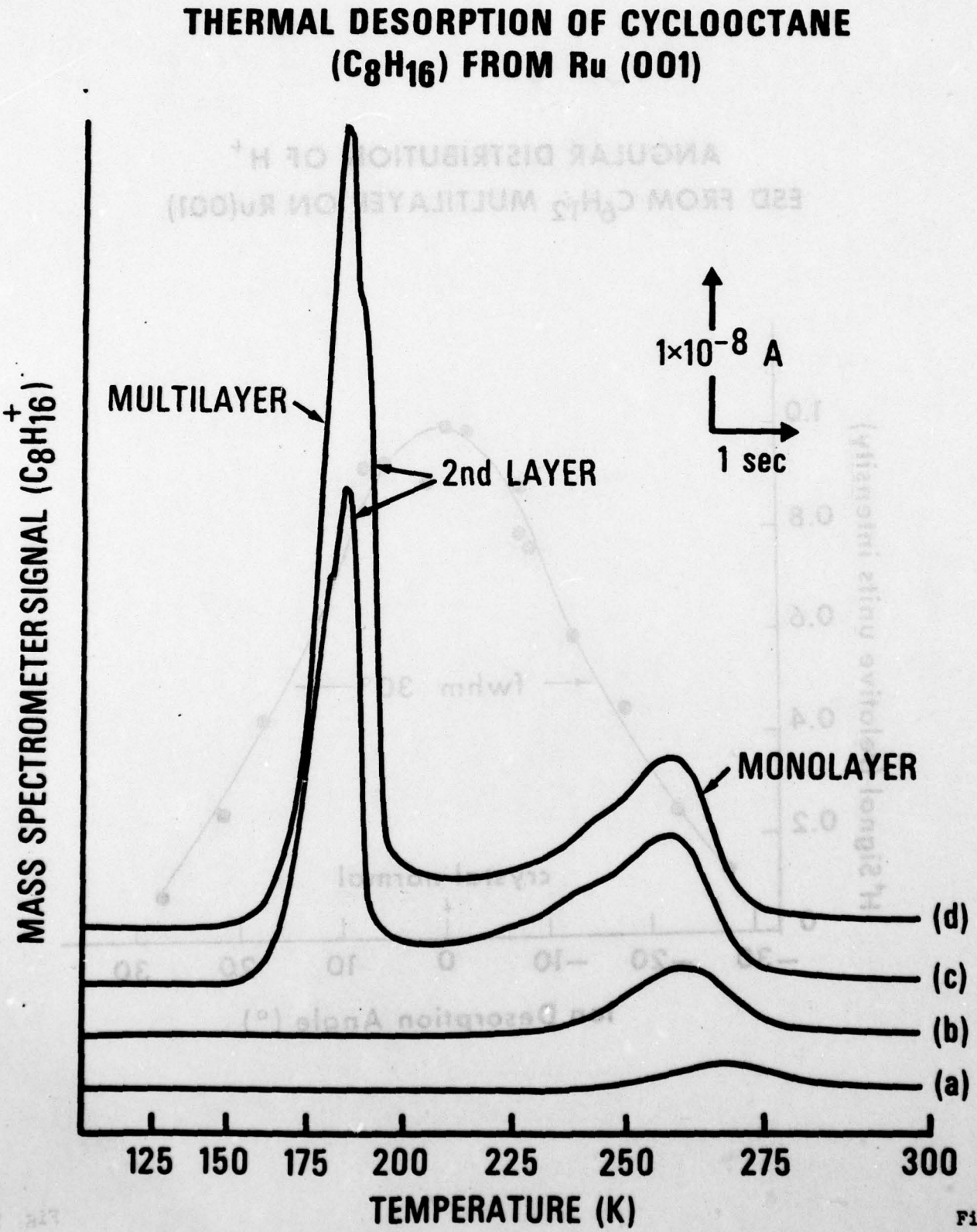
THERMAL DESORPTION OF CYCLOOCTANE
(C_8H_{16}) FROM Ru (001)
MASS SPECTROMETER SIGNAL ($C_8H_{16}^+$)
MULTILAYER
2nd LAYER
MONOLAYER
1×10^{-8} A
1 sec
(d)
(c)
(b)
(a)
125 150 175 200 225 250 275 300
TEMPERATURE (K)

Fig. 10

THERMAL DESORPTION OF HYDROCARBON MONOLAYERS FROM Ru (001)

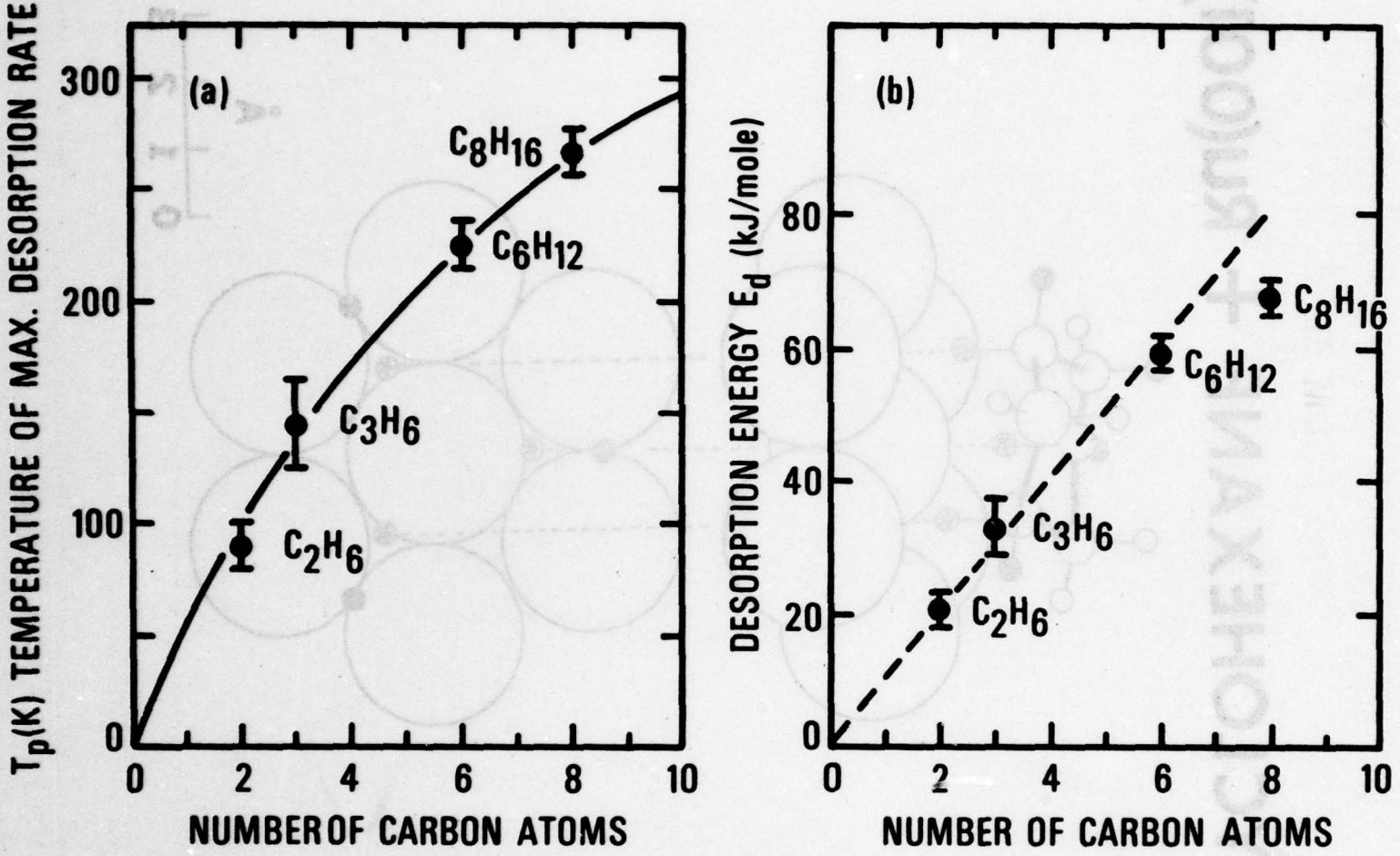

Fig. 11.

CYCLOHEXANE + Ru(001)

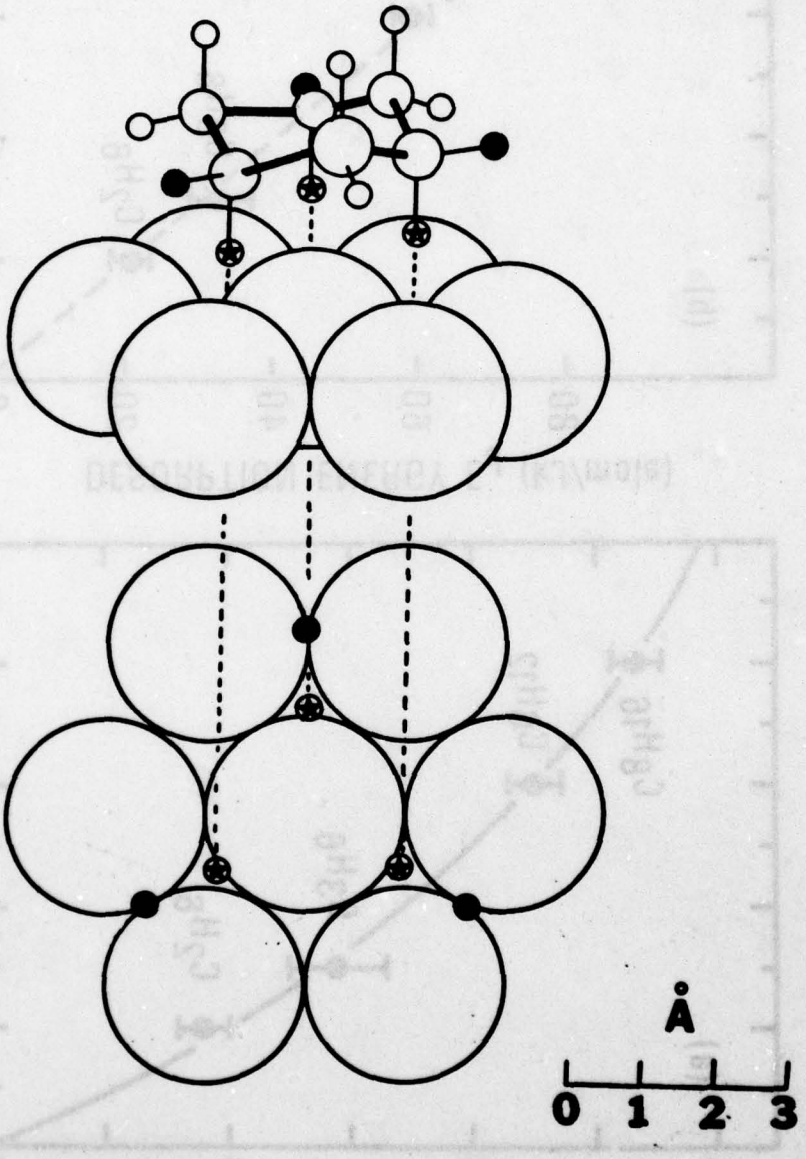

Fig. 12.